iScience

CellPress
OPEN ACCESS

Article

FoxO and rotund form a binding complex governing wing polyphenism in planthoppers

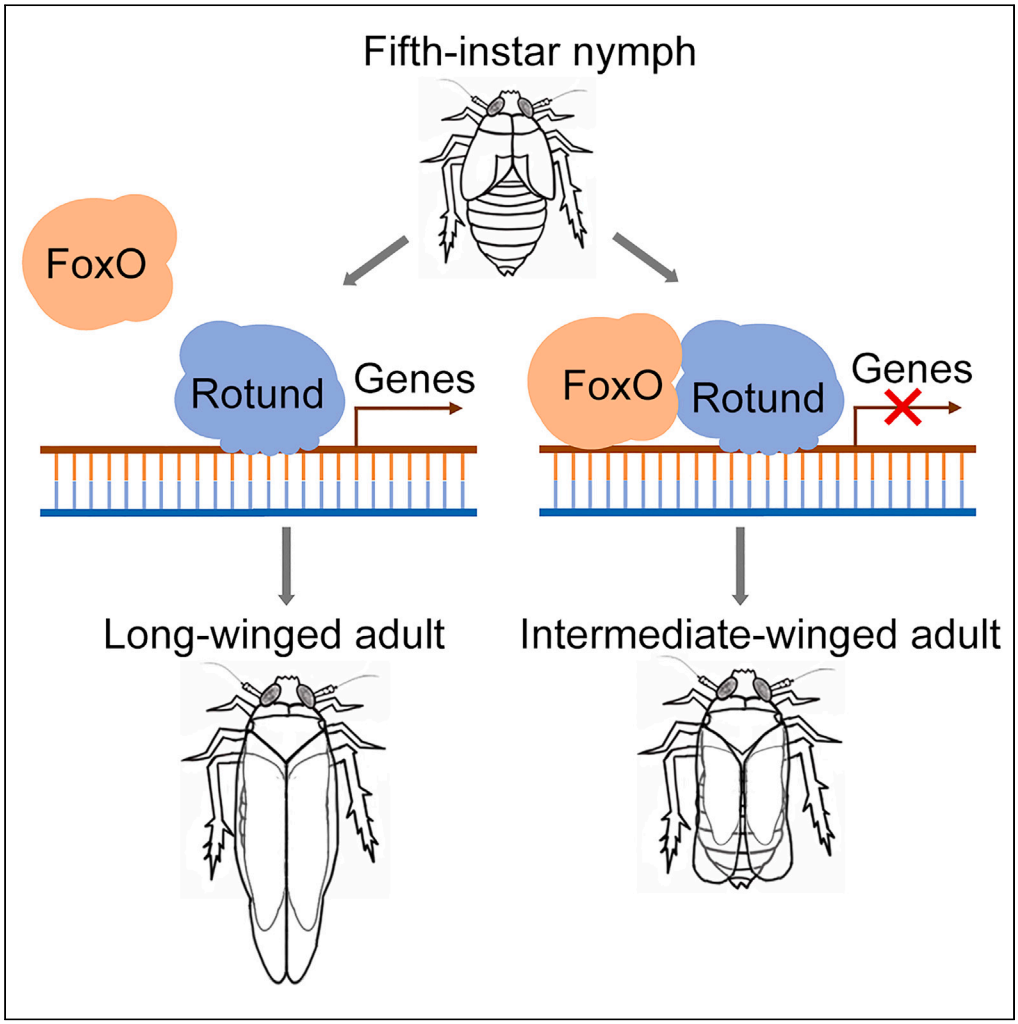

Sun-Jie Chen, Jin-Li Zhang, Wen-Jing Ma, Hui-Jie Wu, Yang Li, Xing-Xing Shen, Hai-Jun Xu

haijunxu@zju.edu.cn

Highlights

Rotund is differentially expressed between long-winged and short-winged BPHs

Knockdown of *rotund* reverses long wings into intermediate wings

Binding to the TF FoxO inhibits the rotund activity

Chen et al., iScience *26*, 107182
July 21, 2023 © 2023 The Author(s).
https://doi.org/10.1016/j.isci.2023.107182

iScience

CellPress
OPEN ACCESS

Article

FoxO and rotund form a binding complex governing wing polyphenism in planthoppers

Sun-Jie Chen,[1,2] Jin-Li Zhang,[1,2] Wen-Jing Ma,[1] Hui-Jie Wu,[1] Yang Li,[1] Xing-Xing Shen,[1] and Hai-Jun Xu[1,3,*]

SUMMARY

Wing polyphenism is found in a variety of insects and offers an attractive model system for studying the evolutionary significance of dispersal. The Forkhead box O (FoxO) transcription factor (TF) acts as a wing-morph switch that directs wing buds developing into long-winged (LW) or short-winged morphs in wing-dimorphic planthoppers, yet the regulatory mechanism of the FoxO module remains elusive. Here, we identified the zinc finger TF rotund as a potential wing-morph regulator via transcriptomic analysis and phenotypic screening in the brown planthopper, *Nilaparvata lugens*. RNA interference-mediated knockdown of *rotund* antagonized the LW development derived from in the context of *FoxO* depletion or the activation of the insulin/insulin-like growth factor signaling cascade, reversing long wings into intermediate wings. *In vitro* binding assays indicated that rotund physically binds to FoxO to form the FoxO combinatorial code. These findings broaden our understanding of the complexity of transcriptional regulation governing wing polyphenism in insects.

INTRODUCTION

Polyphenism is the ability of a single genome to produce two or more distinct phenotypes in response to environmental cues.[1–3] Wing polyphenism is a dramatic case of polyphenism and occurs in a wide variety of insect groups,[4,5] in which winged, wingless, as well as vestigial-winged adults develop within the same population. Winged individuals have functional wings and hence are suited for long-distance migration, allowing them to escape from deteriorating environments and exploit new habitats; by contrast, wingless or vestigial-winged individuals are flightless, but might outcompete winged individuals by compensating alternative life history traits. Although wing polyphenism offers an attractive model system for studying the evolutionary significance of dispersal, its underlying genetic basis is poorly understood.

Pioneering studies indicated that juvenile hormone (JH) was the main hormone involved in endocrine regulation of wing polyphenism in diverse insect species, yet persuasive direct evidence documenting a functional role of JH in wing polyphenism remains lacking.[3,6] Emerging evidence has indicated that insect wing polyphenism might be regulated by different genes as well as by different gene regulatory networks depending on the taxon under study. For instance, winged or wingless morphs in the citrus aphid *Aphis citricidus* can be mediated by small RNAs (e.g. miR-9b)[7] and transgenerational wing dimorphism in the pea aphid *Acyrthosiphom pisum* might be mediated, in part, by an ecdysone signaling pathway.[8] In the wing-dimorphic brown planthopper (BPH; Figure 1A) *Nilaparvata lugens* (Hemiptera: Delphacidae), the Forkhead box O (FoxO) transcription factor (TF) acts as a master regulator of short-winged (SW) and long-winged (LW) morphs by integrating transcriptional signaling inputs from the zinc finger protein Zfh[19] and post-translational signaling inputs from the insulin/insulin-like growth factor (IGF) signaling (IIS) pathway.[10,11] As a result, inactivation of FoxO directs SW-destined nymphs to develop into LW BPH adults; by contrast, activation of FoxO inhibits wing development, leading to SW morphs. Further studies showed that FoxO regulates wing polyphenism, in part, via targeting genes crucial for cell proliferation[12,13] and wing patterning.[14] FoxO TFs belong to the large family of forkhead proteins which is characterized by the presence of a ~100-residue forkhead DNA-binding domain. Accumulated evidence has indicated that FoxOs are key players in the regulation of cell-fate decisions, such as cell death, cell proliferation, and cell metabolism, in a variety of organisms ranging from the nematode *Caenorhabditis elegans* to mammals.[15] In addition to the transcriptional regulation and post-translational modifications, FoxOs bind to partner proteins including signaling molecules, TFs, and cofactors, making possible the fine-tuning of FoxO activity to activate or repress diverse target genes.[16–21] Despite the pivotal role of FoxO in BPH wing

[1]State Key Laboratory of Rice Biology and Breeding, Key Laboratory of Biology of Crop Pathogens and Insects of Zhejiang Province, Institute of Insect Sciences, College of Agriculture and Biotechnology, Zhejiang University; 866 Yu-Hang-Tang Avenue, Hangzhou 310058, China

[2]These authors contributed equally

[3]Lead contact

*Correspondence: haijunxu@zju.edu.cn

https://doi.org/10.1016/j.isci.2023.107182

This is an open access article under the CC BY-NC-ND license (http://creativecommons.org/licenses/by-nc-nd/4.0/).

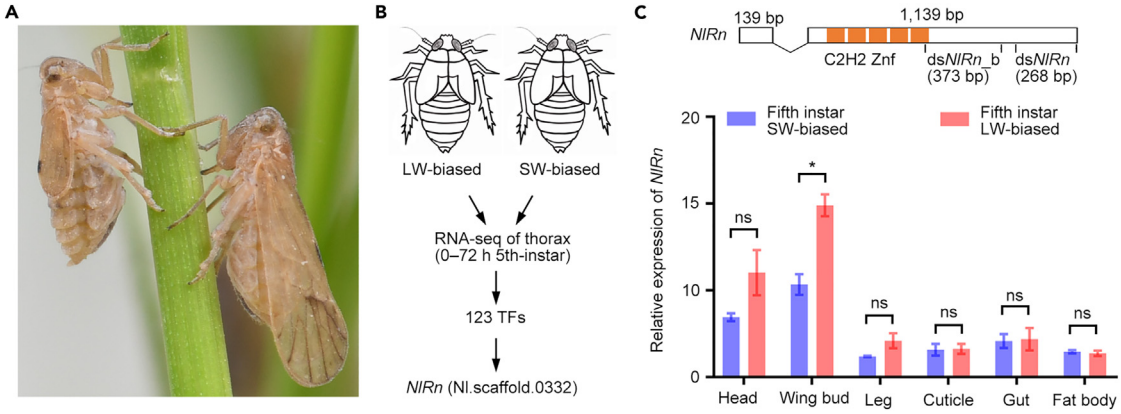

Figure 1. Phenotypic identification and sequence characterization of *NlRn*

(A) Morphology of wild-type short-winged (SW) (left) and long-winged (LW) (right) female adults.

(B) Schematic of the identification of transcription factors (TFs) differentially expressed between LW- and SW-biased nymphs. Thoracic nota (mesonotum and metanotum) dissected from 0 to 72 h fifth-instar nymphs of wild-type SW-biased and LW-biased colonies were used for RNA-sequencing (RNA-seq). Fourth-instar LW-biased nymphs were microinjected with double-stranded RNAs (dsRNAs) targeting each of the 123 differentially expressed TFs. See also Table S1.

(C) Sequence characterization and tissue distribution of *NlRn*. The open reading frame of *NlRn* is split into two exons (139 and 1,139 bp), and contains five C2H2 zinc-finger motifs (orange boxes). Regions targeted by dsRNAs (ds*NlRn* and ds*NlRn*_b) are indicated. To examine the tissue distribution of *NlRn*, various tissues were dissected from fifthinstar LW- and SW-biased nymphs and used for RNA extraction. The relative expression level of *NlRn* was normalized to that of *rps15* via quantitative real-time PCR. Error bars represent mean standard error of the mean (SEM) derived from three independent biological replicates. Statistical comparisons between two groups were performed using two-tailed Student's *t* test, and non-significant (ns) and significant differences (*p = 0.0172) are indicated.

polyphenism, whether and how FoxO-interacting proteins are involved in this process remains to be deciphered.

Here, we identified the *N. lugens* rotund homolog (*Nl*Rn), a conserved C2H2 zinger TF, as a FoxO-binding protein. Binding of FoxO to *Nl*Rn inhibits the *Nl*Rn activity for LW development in BPHs. This finding broadens our understanding of the complexity of transcriptional regulation governing wing polyphenism in insects.

RESULTS

Phenotypic identification of *Nl*Rn

We previously identified 123 TFs that were differentially expressed in thoracic nota of fifth-instar nymphs of LW-biased and SW-biased BPH colonies (Figure 1B). These TFs included two LW-negative regulators (FoxO and Zfh1), knockdown of either of which directed SW-destined nymphs to be LW adults.[9,10] These findings drove us to investigate whether the remaining TFs contained an LW-positive regulator and whether its depletion would result in LW-destined nymphs emerging as SW adults. To this end, fourth-instar (penultimate) LW-biased nymphs were collected for microinjection with double-stranded RNAs (dsRNAs) targeting each of the 123 genes. We noticed that both female and male nymphs treated with dsRNA targeting *NlRn* (ds*NlRn*_b, Figure 1C) exhibited a strong bias toward intermediate-winged (IMW) morphs, relative to control individuals injected with dsRNA targeting the gene encoding green fluorescence protein (ds*Gfp*) (Table S1). Except for *NlRn*, knockdown of the remaining genes led to normal adults with a wing-morph ratio comparable to those microinjected with ds*Gfp*, abnormal adults with curved wings, or lethality.

The open reading frame of *NlRn* is 1,278 bp in length, spliced by two exons (Figure 1C). Analogous to the *Drosophila Rn* homolog, *NlRn* encodes a Krüppel-type zinc finger (Znf) protein containing five C2H2 Znf domains (Figure 1C). To further understand the function of *NlRn*, we used quantitative real-time PCR (qRT-PCR) assays to assess its tissue distribution in fifth-instar (final stage) SW- and LW-biased wild-type (*Wt*) nymphs, the binary decision stage for SW and LW morphs.[14] The results showed that a relatively high number of *NlRn* transcripts were detected in wing buds, but not in other tissues, of fifth-instar LW-biased nymphs compared with fifth-instar SW-biased nymphs (Figure 1C). Thus, these observations indicate that *Nl*Rn might be involved in LW development in BPHs.

NlRn is required for LW development

To confirm the ds*NlRn*_b phenotype, we conducted *NlRn* knockdown using a second non-overlapping dsRNA targeting *NlRn* (ds*NlRn*, Figure 1C). Microinjection of ds*NlRn* significantly reduced the transcriptional level of *NlRn* by 80% compared to the ds*Gfp* treatment (Figure S1). Identical to the ds*NlRn*_b phenotype, most of the LW-biased nymphs challenged with ds*NlRn* developed into female and male adults with intermediate wing size (ds*NlRn*^{IMW}, Figures 2A–2C and S2), compared with SW (ds*Gfp*^{SW}) and LW (ds*Gfp*^{LW}) morphs treated with ds*Gfp*. The IMW morph had forewings and hindwings that did not extend beyond the last abdominal segment, and thus had wings in size between the SW and LW morphs (Figures 2A and 2B). Notably, knockdown of *NlRn* obviously caused cuticle melanization compared with the normal brown cuticle treated with ds*Gfp*. The *Drosophila Rn* homolog is required for normal morphogenesis of specific distal parts of the adult appendages. *Rn* ablation in flies exhibits defects in antennae, proboscis, wings, halters, and three pairs of legs.[22] To investigate the functional specificity of *Nl*Rn, we examined the body size and morphology of eyes and legs. We found that ds*NlRn*^{IMW} BPHs exhibited hind tibia length, a common metric for body size in BPH, comparable to that of ds*Gfp*^{LW} BPHs (Figure 2D), indicating that knockdown of *NlRn* did not change their body size. In addition, ds*NlRn*^{IMW} had eyes (Figure S3) and legs (Figure S4) that were morphologically identical to ds*Gfp*^{LW}, indicating that knockdown of *NlRn* had marginal effects on other tissues except for wings. In addition to ds*NlRn*^{IMW} BPHs, a fraction of SW adults (ds*NlRn*^{SW}) emerged from ds*NlRn*-treated nymphs and had wings that appeared smaller than in those treated with ds*Gfp* (ds*Gfp*^{SW}, Figures 2E and 2F). Together, these results strongly suggested that *Nl*Rn is essential for LW development in BPH.

*Nl*Rn functions oppositely to FoxO

Given that ds*NlRn*^{IMW} adults were derived from LW-biased nymphs and that knockdown of *FoxO* could trigger SW-biased nymphs to become LW morphs, we investigated whether FoxO and *Nl*Rn occur in the same regulatory cascade, but with opposing functions. To this end, we constructed a *FoxO*-null LW BPH colony using CRISPR/Cas9-mediated mutagenesis. A single guide RNA (sgRNA) located at 383–402 nucleotide (nt) downstream of the *FoxO* start codon (ATG) in exon 2 (Figure 3A) was designed for CRISPR/Cas9-mediated mutagenesis of *FoxO*. Pre-blastoderm eggs of SW-biased *Wt* BPHs were collected for microinjection with a mix of sgRNA and Cas9 mRNA, and were then allowed to develop into adults (G0). To obtain a homozygous *FoxO*-null mutant (*FoxO*^{E2}), G0 females were mated with *Wt* males to produce G1 offspring, followed by G1 inbreeding. To verify the genotype of *FoxO*^{E2} mutants, the PCR products spanning the Cas9 cleavage site were amplified from the *FoxO*^{E2} genomic DNA and then directly used for Sanger sequencing. We identified a 4nt-deletion and 14nt-insertion (−4, +14 nt) in *FoxO*^{E2} mutants compared with *Wt* BPHs (Figure 3A), presumably resulting in a frameshift of the coding region of *FoxO* and complete dysfunction of FoxO protein. The *FoxO*^{E2} mutants were 100% LW morphs (Figure 3B), consistent with the *FoxO*-RNA interference (RNAi) phenotype.[10]

To investigate the *NlRn*-RNAi phenotype in the context of *FoxO* depletion, we collected fourth-instar *FoxO*^{E2} nymphs for microinjection with ds*NlRn*. We found that either female or male *FoxO*^{E2} nymphs treated with ds*NlRn* (*FoxO*^{E2}:ds*NlRn*) fully emerged as IMW adults (Figures 3B and 3C) compared with LW morphs treated with ds*Gfp* (*FoxO*^{E2}:ds*Gfp*). In a parallel experiment, we microinjected fourth-instar *FoxO*^{E2} nymphs with a dsRNA targeting *Akt* (ds*Akt*), a key component located upstream of FoxO but downstream of the insulin receptor (InR) pin the IIS pathway.[23] Different from the *NlRn*-RNAi phenotype, knockdown of *Akt* did not alter the *FoxO*^{E2} phenotype because *FoxO*^{E2} nymphs treated with ds*Akt* (*FoxO*^{E2}:ds*Akt*) emerged as LW adults as did those treated with ds*Gfp* (*FoxO*^{E2}:ds*Gfp*, Figures 3B and 3C), suggesting that *Nl*Rn does not act upstream of FoxO as Akt does.

To further confirm the previous phenotype, we performed *NlRn*- and *Akt*-RNAi in the context of *InR2*-null mutants (*NlInR2*^{E4}).[24] InR2 locates upstream of Akt and acts as a negative regulator of the IIS pathway and, as such, *NlInR2*^{E4} mutants are 100% LW morphs because of activation of this pathway. We found that knockdown of either *NlRn* (*NlInR2*^{E4}:ds*NlRn*) or *Akt* (*NlInR2*^{E4}:ds*Akt*) redirected the LW development of *NlInR2*^{E4} mutants into IMW or SW morphs compared with those treated with ds*Gfp* (*NlInR2*^{E4}:ds*Gfp*, Figures 3D and 3E). Thus, we reason that *Nl*Rn was not likely upstream of FoxO in a signaling cascade controlling LW development.

In vitro binding of *Nl*Rn to FoxO

Given that the *Drosophila* Rn homolog was identified as one of several FoxO-interacting proteins in a yeast two-hybrid assay,[25] we hypothesized that BPH FoxO forms a regulatory module by interacting with *Nl*Rn.

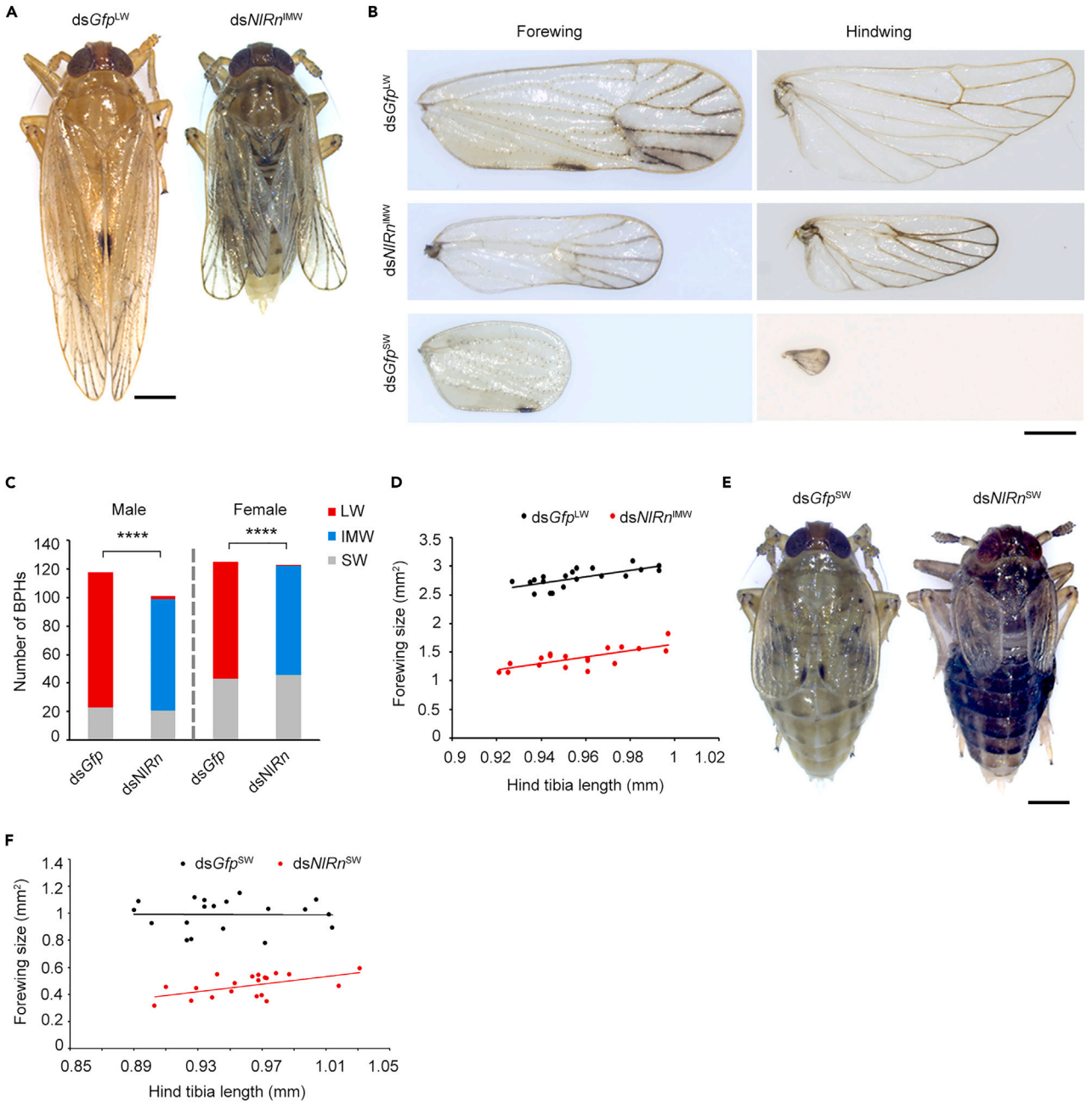

Figure 2. Knockdown of *NlRn* leads to morphs with intermediate-sized wings

(A) Morphology of ds*Gfp*^{LW} and ds*NlRn*^{IMW} females. Four-instar long-winged (LW) biased wild-type nymphs were collected for microinjection with dsRNAs. ds*Gfp*^{LW} indicates ds*Gfp*-treated BPHs with long wings. ds*NlRn*^{IMW} indicates ds*NlRn*-treated BPHs with intermediate-size wings. Scale bar: 500 μm. See also Figure S1.

(B) Morphology of forewings and hindwings of ds*Gfp*^{LW}, ds*NlRn*^{IMW}, and ds*Gfp*^{SW} females. Scale bar: 500 μm.

(C) Number of BPH adults with different wing morphs following dsRNA treatments. Forth-instar LW-biased wild-type nymphs were microinjected with dsRNAs targeting corresponding genes. The LW ratio was compared between the two groups using Pearson χ^2 test (****p = 1.9862E-31, χ^2 = 136.009 and df = 1 for males; ****p = 3.0746E-27, χ^2 = 116.864 and df = 1 for females).

(D) Wing size and hid tibia length in ds*NlRn*^{IMW} and ds*Gfp*^{LW} females. Each dot represents an individual female (n = 20).

(E) Morphology of ds*Gfp*^{SW} and ds*NlRn*^{SW} females. Forth-instar LW-biased nymphs were collected for microinjection with dsRNAs. ds*Gfp*^{SW} and ds*NlRn*^{SW} indicate ds*Gfp*- and ds*NlRn*-treated BPHs with short wings, respectively. Scale bar: 500 μm.

(F) Wing size and hid tibia length in ds*NlRn*^{SW} and ds*Gfp*^{SW} females. Each dot represents an individual female (n = 20).

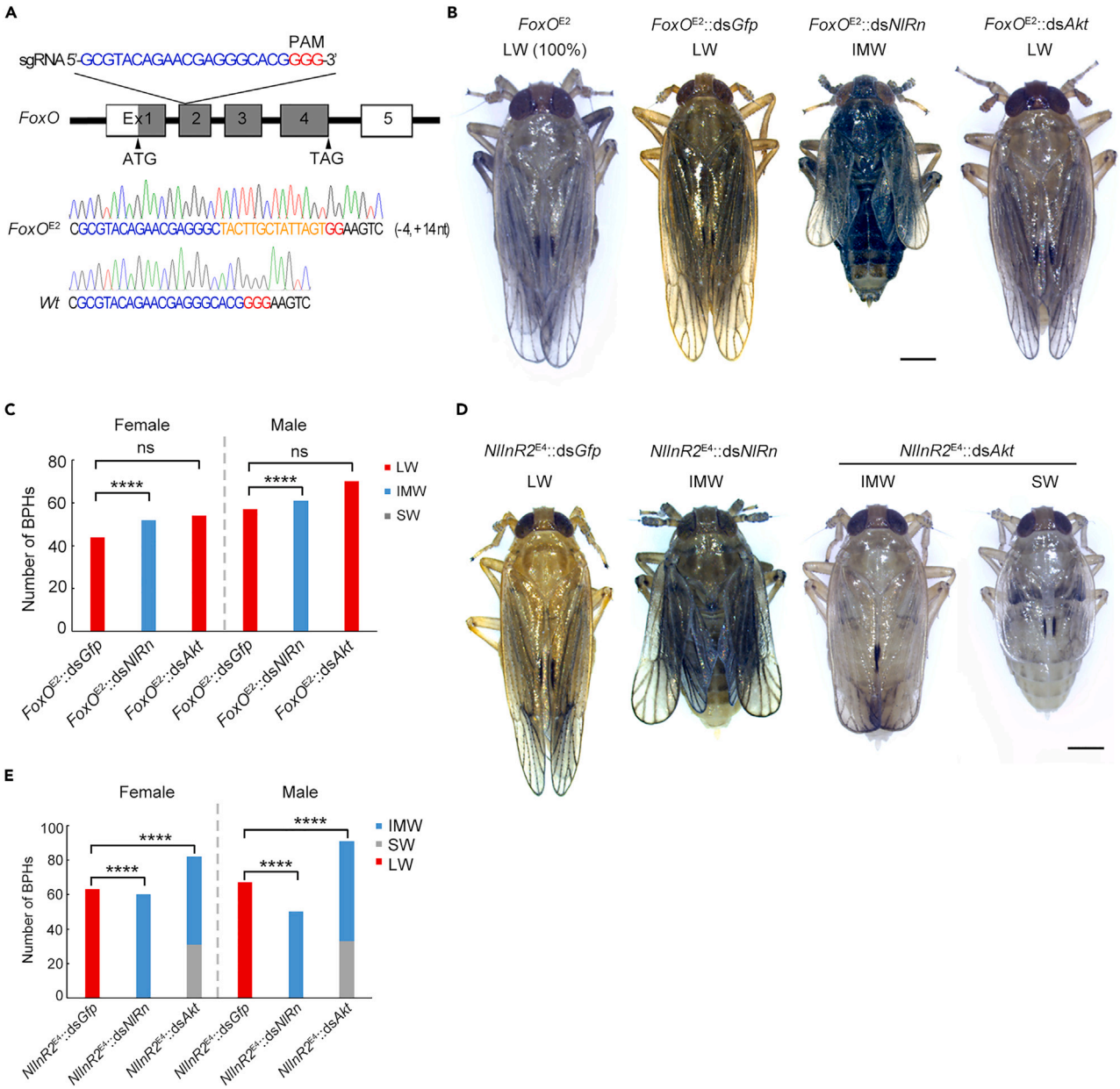

Figure 3. Knockdown of *NlRn* reverses the phenotype derived from *FoxO* and *InR2* depletion

(A) Schematic of the construction of *FoxO* mutants (*FoxO*^{E2}) using CRISPR/Cas9-mediated mutagenesis. The target site for Cas9 and the protospacer-adjacent motif (PAM) are indicated in blue and red, respectively. Exons comprising the *NlRn* cDNA are indicated by numbers, and the encoding region of *NlRn* is indicated by exons in gray. The genotype of *FoxO*^{E2} mutants was confirmed by Sanger sequencing of the region flanking the target site. Exon 2 of *FoxO*^{E2} locus had a 4-nucleotide (nt) deletion and 11-nt insertion (−4, +11).

(B) Morphology of *FoxO*^{E2} female mutants with microinjection of dsRNAs. *FoxO*^{E2} mutants without treatments or microinjected with ds*Gfp* (*FoxO*^{E2}::ds*Gfp*) or ds*Akt* (*FoxO*^{E2}::ds*Akt*) are long-winged (LW) morphs. *FoxO*^{E2} mutants microinjected with ds*NlRn* are intermediate-winged (IMW) morphs. Scale bar: 500 μm.

(C) Number of *FoxO*^{E2} mutants with different wing morphs following dsRNA treatments. Forth-instar *FoxO*^{E2} nymphs were microinjected with dsRNAs targeting corresponding genes. The LW ratio is compared between two groups using Pearson χ^2 test (****p = 1.1488E-22, χ^2 = 96 and df = 1 for females; ****p = 1.7339E-27, χ^2 = 118 and df = 1 for males; ns, not significant).

(D) Morphology of *InR2*^{E4} female mutants following microinjection of dsRNAs. *InR2*^{E4} mutants microinjected with ds*Gfp* are LW morphs. *InR2*^{E4} mutants microinjected with ds*NlRn* or ds*NlAkt* are IMW and SW morphs. Scale bar represents 500 μm.

Figure 3. *Continued*

(E) Number of *InR2*^{E4} mutants with different wing morphs following dsRNA treatments. Forth-instar *InR2*^{E4} nymphs were microinjected with dsRNAs targeting corresponding genes. The LW ratio is compared between two groups using Pearson χ^2 test (for females, ****p = 1.3945E-28, χ^2 = 123 and df = 1 for *InR2*^{E4}:ds*Gfp* vs. *InR2*^{E4}:ds*NlRn*, and ****p = 2.1476E-33, χ^2 = 145 and df = 1 for *InR2*^{E4}:ds*Gfp* vs. *InR2*^{E4}:ds*Akt*; for males, ****p = 2.2807E-27, χ^2 = 117 and df = 1 for *InR2*^{E4}:ds*Gfp* vs. *InR2*^{E4}:ds*NlRn*, and ****p = 3.0949E-36, χ^2 = 158 and df = 1 for *InR2*^{E4}:ds*Gfp* vs. *InR2*^{E4}:ds*Akt*).

To this end, we performed bimolecular fluorescence complementation (BiFC) assays. *NlRn* and *FoxO* were cloned into expression vectors of pCMV-eYfp^N and pCMV-eYfp^C, respectively, each containing the N-terminus (eYfp^N) and C-terminus (eYfp^C) of an enhanced yellow fluorescent reporter protein. Only when the two candidate binding proteins form a pair of interacting partners, the eYfp^N and eYfp^C fold together and generate yellow fluorescence. We observed that yellow fluorescence occurred in HEK293 cells co-transfected with eYfp^N-FoxO and eYfp^C-*Nl*Rn (Figure 4A), but not in cells co-transfected with eYfp^N-FoxO and eYfp^C. To further confirm the binding specificity of *Nl*Rn to FoxO, we performed co-immunoprecipitation (co-IP) assays by co-expressing His-tagged *Nl*Rn (*Nl*Rn-His) with Flag-tagged FoxO (FoxO-Flag) in HEK293 cells. Using anti-Flag monoclonal antibodies, this assay showed that *Nl*Rn-His successfully co-precipitated with FoxO-Flag (Figure 4B). As a negative control, no *Nl*Rn-His was pulled down with anti-Flag antibodies when cells were transfected with a vector expressing *Nl*Rn-His only. In addition, we examined the transcriptional level of *NlRn* in *FoxO*^{E2} or ds*FoxO*-treated fifth-instar nymphs by qRT-PCR. The result showed that depletion of *FoxO* had no significant effects on *NlRn* expression compared with *Wt* BPHs (Figure S5). Taken together, these events suggest that *Nl*Rn antagonizes the FoxO effect in a protein-interacting manner rather than acting as a target of FoxO.

Functional specificity and conservation of *Nl*Rn

Rn proteins form an evolutionarily conserved family of TFs, which have been found in 218 insects representing 11 orders examined, thus far (Figure S6). Interestingly, two *Rn* homologous genes (*Rn* and *Squeeze*) were identified specifically in dipteran insects (e.g., mosquitoes and flies), distinct from one *Rn* homolog in other insect orders. To investigate whether the function of *NlRn* in BPH was conserved in the planthopper family Delphacidae, we performed RNAi-mediated knockdown of *Sogatella furcifera Rn* homolog (*SfRn*), another species representative of wing-dimorphic planthoppers. Analogous to BPHs, microinjection with dsRNA targeting *SfRn* (ds*SfRn*) significantly decreased the LW ratio relative to ds*Gfp* treatment, leading to *S. furcifera* with intermediate-sized wings (Figure 5). This observation indicates that Rn has an evolutionally conserved role in regulating wing polyphenism in insects, at least in the planthopper family Delphacidae.

DISCUSSION

The BPH FoxO is the first identified TF to govern wing polyphenism in insects.[9,10] In addition to BPHs, accumulated reports indicated that FoxO might contribute significantly to wing polyphenism across diverse insect species. For examples, embryonic knockdown of *FoxO* slightly but significantly increased the winged offspring ratio in the pea aphid *Acyrthosiphon pisum*,[26] and the expression level of *FoxO* might be required for soldier-specific morphogenesis in damp-wood termite *Hodotermopsis sjostedti*.[27] FoxOs determine their functional endpoints in part through interacting with a wide variety of unrelated TFs in many organisms.[16,21] To determine wing polyphenism-associated TFs in addition to FoxO, thoracic nota of fifth-instar LW- and SW-biased BPH nymphs were collected for comparative transcriptome analysis, which identified 123 differentially expressed TFs. In our previous study, the TF Zfh1 among the 123 TFs identified was found to govern the development of LW or SW BPHs by transcriptionally regulating the expression level of *FoxO*.[9] In the current study, the TF *Nl*Rn among these 123 TFs were found to physically interact with FoxO and to be indispensable for LW development. This finding sheds new light on how the concerted action of two TFs shapes the developmental plasticity of wing in insects.

Insect *Rn* is required for normal morphogenesis of specific distal parts of adult appendages. For instance, ablation or knockdown of *Rn* induces reduction of the tarsus in the fruit fly *Drosophila melanogaster*,[22] silkworm *Bombyx mori*,[28] and flour beetle *Tribolium castaneum*.[29] However, *Nl*Rn-RNAi BPHs had tarsi that were similar to wild type, coincident with the phenotype derived from the ground beetle *Carabus maiyasanus* with *Rn* knockdown.[30] The simplest interpretation for this distinct phenotype between species might be due to a mild RNAi efficiency in BPHs and *C. maiyasanus*.

In *Drosophila*, *Rn* and *roughened eye* (*roe*) are genetically tightly linked. *Roe* gene is part of *Rn* but is represented by a different transcript resulting from a different promoter. As such, Rn and roe proteins share

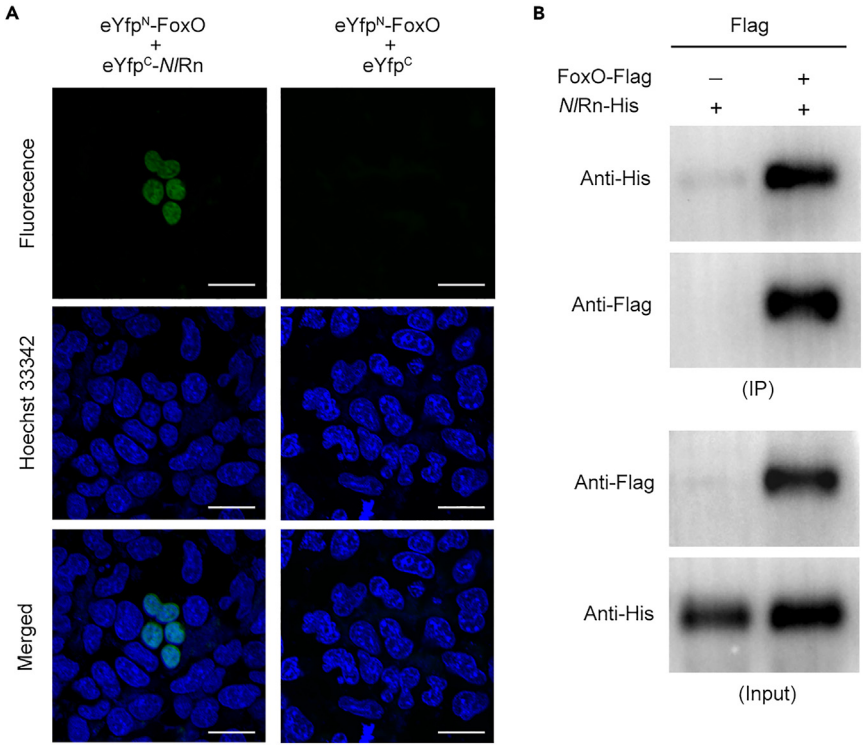

Figure 4. *In vitro* binding assays of *Nl*Rn to FoxO

(A) Identification of *Nl*Rn-FoxO binding by bimolecular fluorescence complementation assays. HEK293 cells were co-transfected with eYfp^{N}-FoxO plus eYfp^{C}-*Nl*Rn or eYfp^{N}-FoxO plus eYfp^{C}. Cells were collected 48 h after transfection for fluorescence examination (green). Cell nucleus was stained with Hoechst 33342 (blue). Scale bar: 20 μm.

(B) Identification of *Nl*Rn-FoxO binding by co-immunoprecipitation assays. HEK293 cells were co-transfected with His-tagged *Nl*Rn (*Nl*Rn-His) with Flag-tagged FoxO (FoxO-Flag). Cell lysates were incubated with anti-Flag magnetic beads, and the eluted proteins were exposed to western blot analysis with anti-His and anti-Flag antibodies.

the same C-terminal region, but differ in their N-terminal regions.[31] *Roe*-mutant flies display rough eye morphology and reduction of photoreceptors.[31,32] In the current study, *NlRn*-RNAi BPH did not exhibit rough eyes even though the ds*NlRn* sequence was designed to target the C-terminal region of *NlRn*, which would degrade transcripts from both *NlRn* and *roe*. Thus, whether the *NlRn* locus contains the *roe* cDNA in BPHs remains to be verified.

The most important finding in the current study was that *NlRn* could partially neutralize the FoxO effect on LW development, leading to both forewings and hindwings with truncated size. This phenotype is reminiscent of truncated wing blades in *Rn*-null flies[33] and shortened elytra in the beetle *C. maiyasanus*.[30] In *Drosophila*, Rn is required for activating and maintaining the expression of *wingless*,[34,35] which encodes a secreted signaling molecule required for many patterning events in both embryonic and postembryonic development.[36] Wingless is required for growth of the wing blade structure in fly wing discs during early larval development,[37,38] while during later larval development, it is involved in bristle patterning along the wing margin.[39] Thus, it is tempting to speculate that activation of FoxO might impair the normal expression of *wingless* by inhibiting the activity of *Nl*Rn. In this scenario, *Nl*Rn might bind DNA directly and the FoxO partner might be recruited to DNA through protein-protein interactions. Although accurate models of gene regulation will require improved understanding of how the FoxO-*Nl*Rn genetic cascade affects the transcriptional specificities of the resulting FoxO module, the result of this study greatly broadens our understanding of the genetically interacting landscape underlying wing polyphenism in insects.

Limitations of the study

Although *in vitro* binding assays indicated that FoxO physically binds to *Nl*Rn, we did not examine the co-location of FoxO and *Nl*Rn in BPH due to the absence of specific antibodies against FoxO and *Nl*Rn.

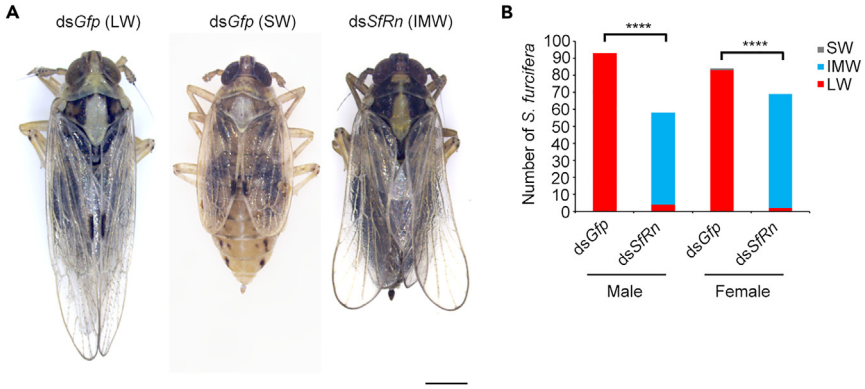

Figure 5. Knockdown of *S. furcifera Rn* homolog (*SfRn*)

(A) Morphology of *S. furcifera* female microinjected with ds*SfRn* or ds*Gfp*. Scale bar: 500 μm.

(B) Number of *S. furcifera* planthoppers with different wing morphs following dsRNA treatments. Forth-instar *S. furcifera* nymphs were microinjected with dsRNAs targeting corresponding genes. The LW ratio was compared between two groups using Pearson χ^2 test (****p = 3.6722E-31, χ^2 = 134.789 and df = 1 for males; ****p = 1.5047E-32, χ^2 = 141.113 and df = 1 for females).

Another caveat of this study is that we did not inspect genomic regions occupied by *Nl*Rn for the DNA-binding site motif of itself and FoxO co-expressed, which would help us understand how two TFs coordinately regulate the expression of target genes.

STAR★METHODS

Detailed methods are provided in the online version of this paper and include the following:

- KEY RESOURCES TABLE
- RESOURCE AVAILABILITY
  - Lead contact
  - Materials availability
  - Data and code availability
- EXPERIMENTAL MODEL AND STUDY PARTICIPANT DETAILS
  - BPH populations
- METHOD DETAILS
  - Gene identification and sequence characterization
  - qRT-PCR
  - dsRNA synthesis and RNAi
  - Synthesis of Cas9 mRNA and sgRNA
  - DNA typing for heterozygosity and homozygosity
  - Embryonic microinjection
  - Crossing scheme
  - BiFC assay
  - Co-IP assay
  - Western blot
  - Image acquisition
- QUANTIFICATION AND STATISTICAL ANALYSIS

SUPPLEMENTAL INFORMATION

Supplemental information can be found online at https://doi.org/10.1016/j.isci.2023.107182.

ACKNOWLEDGMENTS

This work was supported by Development and Demonstration of Comprehensive Technology for Prevention and Control of Major Diseases and Pests (2021YFD1401100), Key Projects of Natural Science Foundation of Zhejiang Province (LZ21C140002), and National Natural Science Foundation of China (32272519 and 32102186).

AUTHOR CONTRIBUTIONS

S.J.C. and H.J.X. designed the research. S.J.C., J.L.Z., and W.J.M. performed the research. S.J.C., Y.L., and X.X.S. analyzed the data. H.J.X. wrote the paper.

DECLARATION OF INTERESTS

The authors declare no competing interests.

INCLUSION AND DIVERSITY

We support inclusive, diverse, and equitable conduct of research.

Received: April 1, 2023
Revised: May 12, 2023
Accepted: June 15, 2023
Published: June 19, 2023

REFERENCES

1. Evans, J.D., and Wheeler, D.E. (2001). Gene expression and the evolution of insect polyphenisms. Bioessays *23*, 62–68. https://doi.org/10.1002/1521-1878(200101)23:1<62::AID-BIES1008>3.0.CO;2-7.

2. Smith, C.R., Toth, A.L., Suarez, A.V., and Robinson, G.E. (2008). Genetic and genomic analyses of the division of labour in insect societies. Nat. Rev. Genet. *9*, 735–748. https://doi.org/10.1038/nrg2429.

3. Simpson, S.J., Sword, G.A., and Lo, N. (2011). Polyphenism in Insects. Curr. Biol. *21*, R738–R749. https://doi.org/10.1016/j.cub.2012.01.051.

4. Roff, D.A. (1994). The evolution of flightlessness: is history important? Evol. Ecol. *8*, 639–657. https://doi.org/10.1007/BF01237847.

5. Zera, A.J. (2009). Wing polymorphism in *Gryllus* (Orthoptera: Gryllidae): proximate endocrine, energetic and biochemical mechanisms underlying morph specialization for flight vs. reproduction. In Phenotypic Plasticity of Insects: Mechanisms and Consequences, D.W. Whitman and T.N. Ananthakrishnan, eds. (Enfield, NH: Sci. Publ.), pp. 609–653.

6. Zhang, C.X., Brisson, J.A., and Xu, H.J. (2019). Molecular mechanisms of wing polymorphism in insects. Annu. Rev. Entomol. *64*, 297–314. https://doi.org/10.1146/annurev-ento-011118-112448.

7. Shang, F., Niu, J., Ding, B.Y., Zhang, W., Wei, D.D., Wei, D., Jiang, H.B., and Wang, J.J. (2020). The miR-9b microRNA mediates dimorphism and development of wing in aphids. Proc. Natl. Acad. Sci. USA *117*, 8404–8409. https://doi.org/10.1073/pnas.1919204117.

8. Vellichirammal, N.N., Gupta, P., Hall, T.A., and Brisson, J.A. (2017). Ecdysone signaling underlies the pea aphid transgenerational wing polyphenism. Proc. Natl. Acad. Sci. USA *114*, 1419–1423. https://doi.org/10.1073/pnas.1617640114.

9. Zhang, J.L., Chen, S.J., Liu, X.Y., Moczek, A.P., and Xu, H.J. (2022). The transcription factor Zfh1 acts as a wing-morph switch in planthoppers. Nat. Commun. *13*, 5670. https://doi.org/10.1038/s41467-022-33422-6.

10. Xu, H.J., Xue, J., Lu, B., Zhang, X.C., Zhuo, J.C., He, S.F., Ma, X.F., Jiang, Y.Q., Fan, H.W., Xu, J.Y., et al. (2015). Two insulin receptors determine alternative wing morphs in planthoppers. Nature *519*, 464–467. https://doi.org/10.1038/nature14286.

11. Lin, X., Yao, Y., Wang, B., Emlen, D.J., and Lavine, L.C. (2016). Ecological trade-offs between migration and reproduction are mediated by the nutrition-sensitive insulin-signaling pathway. Int. J. Biol. Sci. *12*, 607–616. https://doi.org/10.7150/ijbs.14802.

12. Lin, X., Gao, H., Xu, Y., Zhang, Y., Li, Y., Lavine, M.D., and Lavine, L.C. (2020). Cell cycle progression determines wing morph in the polyphonic insect *Nilaparvata lugens*. iScience *23*, 101040. https://doi.org/10.1016/j.isci.2020.101040.

13. Xu, N., Wei, S.F., and Xu, H.J. (2021). Transcriptome analysis of the regulatory mechanism of FoxO on wing dimorphism in the brown planthopper, *Nilaparvata lugens* (Hemiptera: Delphacidae). Insects *12*, 413. https://doi.org/10.3390/insects12050413.

14. Zhang, J.L., Fu, S.J., Chen, S.J., Chen, H.H., Liu, Y.L., Liu, X.Y., and Xu, H.J. (2021). *Vestigial* mediates the effect of insulin signaling pathway on wing-morph switching in planthoppers. PLoS Genet. *17*, e1009312. https://doi.org/10.1371/journal.pgen.1009312.

15. Burgering, B.M.T. (2008). A brief introduction to FOXOlogy. Oncogene *27*, 2258–2262. https://doi.org/10.1038/onc.2008.29.

16. Calnan, D.R., and Brunet, A. (2008). The FoxO code. Oncogene *27*, 2276–2288. https://doi.org/10.1038/onc.2008.21.

17. Daitoku, H., Sakamaki, J.I., and Fukamizu, A. (2011). Regulation of FoxO transcription factors by acetylation and protein-protein interactions. Biochim. Biophys. Acta *1813*, 1954–1960. https://doi.org/10.1016/j.bbamcr.2011.03.001.

18. Kodani, N., and Nakae, J. (2020). Tissue-specific metabolic regulation of FOXO-binding protein: FOXO does not act alone. Cells *9*, 702. https://doi.org/10.3390/cells9030702.

19. Myatt, S.S., and Lam, E.W.F. (2007). The emerging roles of forkhead box (Fox) proteins in cancer. Nat. Rev. Cancer *7*, 847–859. https://doi.org/10.1038/nrc2223.

20. Ramaswamy, S., Nakamura, N., Sansal, I., Bergeron, L., and Sellers, W.R. (2002). A novel mechanism of gene regulation and tumor suppression by the transcription factor FKHR. Cancer Cell *2*, 81–91. https://doi.org/10.1016/s1535-6108(02)00086-7.

21. van der Vos, K.E., and Coffer, P.J. (2008). FOXO-binding partners: it takes two to tango. Oncogene *27*, 2289–2299. https://doi.org/10.1038/onc.2008.22.

22. Kerridge, S., and Thomas-Cavallin, M. (1988). Appendage morphogenesis in *Drosophila*: a developmental study of the rotund (rn) gene. Dev. Biol. *197*, 19–26. https://doi.org/10.1007/BF00376037.

23. Taniguchi, C.M., Emanuelli, B., and Kahn, C.R. (2006). Critical nodes in signalling pathways: insights into insulin action. Nat. Rev. Mol. Cell Biol. *7*, 85–96. https://doi.org/10.1038/nrm1837.

24. Xue, W.H., Xu, N., Chen, S.J., Liu, X.Y., Zhang, J.L., and Xu, H.J. (2021). Neofunctionalization of a second insulin receptor gene in the wing-dimorphic planthopper, *Nilaparvata lugens*. PLoS Genet. *17*, e1009653. https://doi.org/10.1371/journal.pgen.1009653.

25. Shokri, L., Inukai, S., Hafner, A., Weinand, K., Hens, K., Vedenko, A., Gisselbrecht, S.S., Dainese, R., Bischof, J., Furger, E., et al. (2019). A comprehensive *Drosophila melanogaster* transcription factor interactome. Cell Rep. *27*, 955–970.e7. https://doi.org/10.1016/j.celrep.2019.03.071.

26. Yuan, Y., Wang, Y., Ye, W., Yuan, E., Di, J., Chen, X., Xing, Y., Sun, Y., and Ge, F. (2023). Functonal evaluation of the insulin/insulin-like growth factor signaling pathway in determination of wing polyphenism in pea aphid. Insect Sci. *30*, 816–828. https://doi.org/10.1111/1744-7917.13121.

27. Hattori, A., Sugime, Y., Sasa, C., Miyakawa, H., Ishikawa, Y., Miyazaki, S., Okada, Y., Cornette, R., Lavine, L.C., Emlen, D.J., et al. (2013). Soldier morphogenesis in the damp-wood terminte is regulated by the insulin signaling pathway. J. Exp. Zool. *320*, 295–306. https://doi.org/10.1002/jez.b.22501.

28. Zhou, C.Y., Zha, X.F., Liu, H.W., and Xia, Q.Y. (2017). Zinc finger protein rotund deficiency affects development of the thoracic leg in Bombyx mori. Insect Sci. *24*, 385–396. https://doi.org/10.1111/1744-7917.12334.

29. Angelini, D.R., Smith, F.W., and Jockusch, E.L. (2012). Extent with modification: leg patterning in the beetle *Tribolium castaneum* and the evolution of serial homologs. G3 *2*, 235–248. https://doi.org/10.1534/g3.111.001537.

30. Sota, T., Sugawara, H., Fujisawa, T., Fujimaki, K., and Niimi, T. (2018). Knockdown of *rotund* gene through larval RNA interference affects genital and elytral morphology in the ground beetle *Carabus maiyasanus* (Coleoptera: Carabidae). Entomol. Sci. *21*, 469–474. https://doi.org/10.1111/ens.12330.

31. Renfranz, P.J., and Benzer, S. (1989). Monoclonal antibody probes discriminate early and late mutant defects in development of the *Drosophila retina*. Dev. Biol. *136*, 411–429. https://doi.org/10.1016/0012-1606(89)90267-4.

32. St Pierre, S.E., Galindo, M.I., Couso, J.P., and Thor, S. (2002). Control of *Drosophila* imaginal disc development by *rotund* and *roughened eye*: differentially expressed transcripts of the same gene encoding functionally distinct zinc finger proteins. Development *129*, 1273–1281. https://doi.org/10.1242/dev.129.5.1273.

33. Cavener, D.R., Otteson, D.C., and Kaufman, T.C. (1986). A rehabilitation of the genetic map of the 84B-D region in *Drosophila melanogaster*. Genetics *114*, 111–123. https://doi.org/10.1093/genetics/114.1.111.

34. Rodríguez Dd, D.d.A., Terriente, J., Galindo, M.I., Couso, J.P., and Díaz-Benjumea, F.J. (2002). Different mechanisms initiate and maintain *wingless* expression in the *Drosophila* wing hinge. Development *129*, 3995–4004. https://doi.org/10.1242/dev.129.17.3995.

35. Terriente Félix, J., Magariños, M., and Díaz-Benjumea, F.J. (2007). Nab controls the activity of the zinc-finger transcription factors Squeeze and Rotund in *Drosophila* development. Development *134*, 1845–1852. https://doi.org/10.1242/dev.003830.

36. Cadigan, K.M., and Nusse, R. (1996). *wingless* signaling in the *Drosophila* eye and embryonic epidermis. Development *122*, 2801–2812. https://doi.org/10.1242/dev.122.9.2801.

37. Morata, G., and Lawrence, P.A. (1977). The development of wingless, a homeotic mutation of *Drosophila*. Dev. Biol. *56*, 227–240. https://doi.org/10.1016/0012-1606(77)90266-4.

38. Williams, J.A., Paddock, S.W., and Carroll, S.B. (1993). Pattern formation in a secondary field: a hierarchy of regulatory genes subdivides the developing *Drosophila* wing disc into discrete subregions. Development *117*, 571–584. https://doi.org/10.1242/dev.117.2.571.

39. Phillips, R.G., and Whittle, J.R. (1993). *wingless* expression mediates determination of peripheral nervous system elements in late stages of *Drosophila* wing disc development. Development *118*, 427–438. https://doi.org/10.1242/dev.118.2.427.

40. Li, Y., Liu, Z., Liu, C., Shi, Z., Pang, L., Chen, C., Chen, Y., Pan, R., Zhou, W., Chen, X.X., et al. (2022). HGT is widespread in insects and contributes to male courtship in lepidopterans. Cell *185*, 2975–2987.e10. https://doi.org/10.1016/j.cell.2022.06.014.

41. Yuan, M., Lu, Y., Zhu, X., Wan, H., Shakeel, M., Zhan, S., Jin, B.R., and Li, J. (2014). Selection and evaluation of potential reference genes for gene expression analysis in the brown planthopper, *Nilaparvata lugens* (Hemiptera: Delphacidae) using reverse-transcription quantitative PCR. PLoS One *9*, e86503. https://doi.org/10.1371/journal.pone.0086503.

42. Livak, K.J., and Schmittgen, T.D. (2001). Analysis of relative gene expression data using real-time quantitative PCR and the 2-ΔΔCT method. Methods *25*, 402–408. https://doi.org/10.1006/meth.2001.1262.

43. Xu, H.J., Chen, T., Ma, X.F., Xue, J., Pan, P.L., Zhang, X.C., Cheng, J.A., and Zhang, C.X. (2013). Genome-wide screening for components of small interfering RNA (siRNA) and micro-RNA (miRNA) pathways in the brown planthopper, *Nilaparvata lugens* (Hemiptera: Delphacidae). Insect Mol. Biol. *22*, 635–647. https://doi.org/10.1111/imb.12051.

44. Xue, W.H., Xu, N., Yuan, X.B., Chen, H.H., Zhang, J.L., Fu, S.J., Zhang, C.X., and Xu, H.J. (2018). CRISPR/Cas9-meidated knockout of two eye pigmentation genes in the brown planthopper, *Nilaparvata lugens* (Hemiptera: Delphacidae). Insect Biochem. Mol. Biol. *93*, 19–26. https://doi.org/10.1016/j.ibmb.2017.12.003.

45. Reding, K., and Pick, L. (2020). High-efficiency CRISPR/Cas9 mutagenesis of the white gene in the milkweed bug *Oncopeltus fasciatus*. Genetics *215*, 1027–1037. https://doi.org/10.1534/genetics.120.303269.

STAR★METHODS

KEY RESOURCES TABLE

REAGENT or RESOURCE	SOURCE	IDENTIFIER
Antibodies		
HRP-conjugated anti-Flag (Mouse)	MBL	Cat#M185-7; RRID:AB_2687989
HRP-conjugated anti-His (Mouse)	Proteintech	Cat#HRP-66005; RRID:AB_2857904
Biological samples		
Brown planthopper (LW-biased population)	Huazhong Agricultural University, China	LW
Brown planthopper (SW-biased population)	Hangzhou, China	SW
Planthopper mutants (*FoxO*^{E2})	This paper	*FoxO*^{E2}
Planthopper mutants (*NlInR2*^{E4})	Dr. Hai-Jun Xu	Xue et al.[24]
Rice, *Oryza sativa*	Jiaxing Academy of Agricultural Sciences	Xiushui 11
Chemicals, peptides and recombinant proteins		
RNAiso Plus	TaKaRa	Cat#9109
HiScript QRT SuperMix	Vazyme	Cat#R122-01
fidelity DNA polymerase	Vazyme	Cat#P505-d1
T7 high-yield transcription kit	Vazyme	Cat#TR101-01
the mMESSAGE mMACHINE SP6 transcription kit	Thermo Fisher Scientific	Cat#AM1340
Poly(A) tailing kit	Thermo Fisher Scientific	Cat#AM1350
pEasy-T3 cloning vector	TransGen Biotech	Cat#CT301-01
Flag-M2 magnetic beads	Sigma	Cat#M8832
Dulbecco's Modified Eagle's Medium	Sangon	Cat#E600003
10% fetal bovine serum	Gibco	Cat#10099141
liposomal transfection reagent	Yeasen	Cat#40802ES01
Immobilon-P transfer membrane	Immobilon	Cat#IPVH00010
Critical commercial assays		
ChemiDoc XRS + system	Bio-Rad	Cat#1708265
CFX96 real-time PCR detection system	Bio-Rad	Cat#1845097
Zeiss LSM 800 confocal microscope	Carl Zeiss MicroImaging	Cat#400102-9010
LEICA S8AP0 stereomicroscope	LEICA	Cat#10450703
Tabletop Microscope TM-1000	Hitachi	Cat#0503-05
Deposited data		
RNA sequencing data	Dr. Hai-Jun Xu	GenBank: PRJNA805395
Experimental models: Cell lines		
HEK293T cells lines	Dr. Naiming Zhou	Zhou's Lab (College of Life Sciences, Zhejiang University, China)
Oligonucleotides		
dsRNA primers	This study	Table S2
qRT-PCR primers	This study	Table S2
sgRNA primers	This study	Table S2
DNA amplication primers	This study	Table S2
Recombinant DNA		
pCMV-eYfp^{N}-FoxO	This study	N/A
pCMV-eYfp^{C}-*Nl*Rn	This study	N/A

(*Continued on next page*)

Continued

REAGENT or RESOURCE	SOURCE	IDENTIFIER
pcDNA3.1-FoxO-Flag	This study	N/A
pcDNA3.1-*Nl*Rn-His	This study	N/A
Software and algorithms		
ImageJ	National Institutes of Health	RRID: SCR_003070
GraphPad Prism	GraphPad Software Inc	RRID: SCR_002798
SPSS	SPSS Inc	RRID:SCR_002865

RESOURCE AVAILABILITY

Lead contact

Further information and requests for resources, reagents and strains should be directed to and will be fulfilled by the lead contact, Hai-Jun Xu (haijunxu@zju.edu.cn).

Materials availability

This study did not generate new unique reagents. All key resources are listed in the key resources table. Further information and requests for resources and reagents should be directed to the lead contact.

Data and code availability

- All data are available in the manuscript or the supplementary data. The RNA sequencing data generated from LW- and SW-biased nymphs is available under the GenBank: PRJNA805395. The *NlRn* sequence is publically available under the GenBank: XM_039435512.
- This paper does not report original code.
- Any additional information required to reanalyze the data reported in this paper is available from the lead contact upon request.

EXPERIMENTAL MODEL AND STUDY PARTICIPANT DETAILS

BPH populations

The SW-biased *N. lugens* population (SW ratio ~95% ± 5%) and the planthopper *S. furcifera* (LW ratio ~99% ± 1%) were established from colonies collected in Hangzhou, China, in 2008. The LW-biased *N. lugens* population (LW ratio ~60% ± 10%) was provided by Dr. Hong-Xia Hua (Huazhong Agricultural University, China). BPHs (~ 5000 individuals) were kept in nylon mesh containers (L: W: H = 45cm: 40cm: 40cm). BPHs challenged with dsRNAs were kept in round plastic jars (7cm diameter and 10cm height). All BPHs were allowed to feed on rice seedlings (rice variety: Xiushui 11) at 26 ± 0.5°C, with 50 ± 5% relative humidity under a photoperiod of 16:8 h (L:D).

BPHs were considered as the LW morph if both forewings and hind wings extended beyond the tip of the abdomen. We defined BPHs as the SW morph if forewings and hindwings extended no more than the sixth and first abdominal segment, respectively. We defined BPHs as the IMW morph if both forewings and hind wings did not extend beyond the last abdominal segment.

METHOD DETAILS

Gene identification and sequence characterization

Total RNAs were isolated from BPH adults using RNAiso Plus (TaKaRa, 9109). For cDNA syntheses, 900 ng of total RNA was reversely transcribed in a 20 μl reaction with HiScript QRT SuperMix (Vazyme, R122-01). The full open reading frame of *NlRn* was amplified from cDNA using fidelity DNA polymerase (Vazyme, P505-d1) with NlRn-orf-F and NlRn-orf-R (Table S2). The PCR product was cloned and the sequence was determined by Sanger sequencing. The *NlRn* sequence is identical to the one publically available in GenBank (XM_039435512). A phylogenetic tree was constructed as reported in our previous study.[40] Images representing taxa were taken from PhyloPic (http://phylopic.org). To examine the tissue distribution of *NlRn*, the head, fat body, gut, wing buds, legs, and cuticle were dissected from fifth-instar nymphs

(n = 50) and used for RNA extraction. Three independent biological replicates were used for RNA isolation, and first-strand cDNA was synthesized for quantification of *NlRn* expression via qRT-PCR.

qRT-PCR

Total RNAs were isolated from samples using RNAiso Plus (TaKaRa, 9109). First-strand cDNA was synthesized using HiScript QRT SuperMix (Vazyme, R122-01). qRT-qPCR was performed on a CFX96 real-time PCR detection system (Bio-Rad, Hercules, CA, USA) with the following conditions: denaturation for 3 min at 95°C, followed by 40 cycles at 95°C for 10 s, and 60°C for 30 s. The expression levels of target genes were normalized by the gene encoding ribosomal protein S15 (*rps15*)[41] using the $2^{-\Delta\Delta CT}$ method.[42] Specific primers for each target gene were listed in Table S2. Each sample was loaded for qRT-PCR assays with three technical replicates. Data used for statistical analysis were derived from three biological replicates.

dsRNA synthesis and RNAi

The synthesis and injections of dsRNA were performed as previously reported.[10,43] Briefly, dsRNAs were synthesized using a T7 high-yield transcription kit (Vazyme, TR101-01) according to the manufacturer's instructions. The dsRNA primers targeting corresponding genes were synthesized with the T7 RNA polymerase promoter at both ends (Table S2). Fourth-instar nymphs were anaesthetized with carbon dioxide for 30 s, and ~150 ng dsRNA was injected into the mesothorax using a FemtoJet microinjection system (Eppendorf, Hamburg, Germany). In parallel, microinjection of ds*Gfp* was set as a control. The RNAi efficiency was examined by qRT-PCR 72 h after microinjection.

Synthesis of Cas9 mRNA and sgRNA

The sgRNAs were searched in the BPH genome using the *FoxO* sequence on the Guide Design Resources website (https://zlab.bio/guide-design-resources). The sgRNAs were prepared as previously described[44] with transcription performed using a T7 high-yield transcription kit (Vazyme, TR101-01) according to the manufacturer's instructions. Cas9 mRNA was *in vitro* transcribed from a plasmid pSP6-2sNLS-SpCas9 vector using the mMESSAGE mMACHINE SP6 transcription kit (Thermo Fisher Scientific, AM1340) and Poly(A) tailing kit (Thermo Fisher Scientific, AM1350) according to the manufacturer's instructions.

DNA typing for heterozygosity and homozygosity

Isolation of genomic DNA (gDNA) from whole BPH bodies was performed as reported previously.[45] Briefly, a single adult was homogenized in a 1.5 ml Eppendorf tube, followed by the addition of 100 μl of extraction buffer (10 mM Tris-HCl pH 8.2, 1 mM EDTA, 25 mM NaCl, 0.2 mg/ml proteinase K). The tubes were incubated for 30 min at 37°C, followed by 2 min at 95°C to inactivate proteinase K, and the supernatant solution was used directly as a template for PCR assays. Isolation of gDNA from wings was performed as previously described with small modifications.[24] Briefly, forewings were digested in 0.5 ml extraction buffer [0.01 M Tris-HCl, 0.01 M EDTA, 0.1 M NaCl, 0.039 M dithiothreitol (DTT), 2% sodium dodecyl sulfate, 20 μg/ml, pH 8.0] for 12 h at 37°C, and then precipitated with isopropanol. The gDNA was used as a template for PCR assays with specific primers $FoxO^{E2}$-test-F/R (Table S2) for sgRNA target sites. The PCR products were then directly used for Sanger sequencing or subcloned into pEasy-T3 cloning vector (TransGen Biotech, CT301-01), and single clones were then picked for Sanger sequencing.

Embryonic microinjection

Embryonic microinjection was performed as reported previously.[44] SW-biased females were allowed to lay eggs for 1 h. Pre-blastoderm eggs were collected within 1 h of oviposition, and microinjection manipulation was accomplished in the following 1 h. Individual eggs were injected with a mix (0.5 nl) of Cas9 mRNA (500 ng/μl) and *FoxO* sgRNA (150 ng/μl). After microinjection, eggs were placed in a walk-in chamber at 26 ± 0.5°C with a 16: 8 h (light: dark) photoperiod and relative humidity of 50 ± 5%. The hatched nymphs were transferred immediately to fresh rice seedlings.

Crossing scheme

A homozygous mutant line was obtained via cross-mating as previously described.[44] A single CRISPR/Cas9-injected G0 female was allowed to mate with one *Wt* male to produce G1 progeny, and G0 females were then homogenized for genotyping. To determine the genotype of G1 progeny, gDNA isolated from wings was used for PCR assays, as described above. A single G1 adult was allowed to mate with one *Wt* adult to produce G2 progeny. A homozygous mutant population was derived by G2 self-crossing.

BiFC assay

Two BiFC constructs, pCMV-eYfp^N and pCMV-eYfp^C, contain each a complementary fragment of a fluorescent reporter protein. *FoxO* and *NlRn* were subcloned into pCMV-eYfp^N and pCMV-eYfp^C to produce eYfp^N-FoxO and eYfp^C-*Nl*Rn recombinant vectors, respectively. HEK293T cells were cultured in 30mm-diameter plates containing Dulbecco's Modified Eagle's Medium (Sangon, E600003) with 10% fetal bovine serum (Gibco, 10099141) at 37°C under 5% CO_2. HEK293T cells were co-transfected with eYfp^N-FoxO and eYfp^C-*Nl*Rn (0.5 μg of each plasmid) using liposomal transfection reagent (Yeasen, 40802ES01). Cells co-transfected with eYfp^N-FoxO and a vector only (eYfp^C) severed as a control. Then, 48 h after transfection, cells were washed three times with phosphate buffer saline (PBS) and stained with Hoechst 33342 (5 μg/ml) for 30 min. Fluorescent images were acquired using a Zeiss LSM 800 confocal microscope (Carl Zeiss MicroImaging, Göttingen, Germany).

Co-IP assay

HEK293T cells in 30mm-diameter plates were transfected with Flag-tagged pcDNA3.1-FoxO plus His-tagged pcDNA3.1-*Nl*Rn. Then, 48 h after transfection, the cells were rinsed with cold PBS for three times and then homogenized in NETN buffer (25mM Tis-HCl pH 8.0, 100 mM NaCl, 1 mM EDTA, 0.5 mM DTT, 0.5% NP-40) with protease inhibitor cocktail. Lysates were cleared by centrifugation at 16,000*g* for 15 min at 4°C, and the supernatant was then incubated with Flag-M2 magnetic beads (Sigma, M8832) at 4°C for 3 h with gentle rotation. The beads were washed five times with cold NETN buffer, followed by elution with 2 × SDS-PAGE loading buffer. Equal amounts of samples were loaded on SDS-PAGE gels, followed by western blot analysis.

Western blot

Proteins were separated by 10% SDS-PAGE and then transferred onto an Immobilon-P transfer membrane (Immobilon, IPVH00010). The proteins were incubated with either HRP-conjugated anti-Flag (MBL, M185-7, 1:5000) or HRP-conjugated anti-His (Proteintech, HRP-66005, 1:10000) antibodies for 1 h at room temperature. Immunoreactivity was imaged with the Molecular Imager ChemiDoc XRS + system (Bio-Rad, Hercules, CA, USA).

Image acquisition

Images of insect bodies, forewings, and hid tibias were captured using a DFC320 digital camera attached to a LEICA S8AP0 stereomicroscope (LEICA, Wetzlar, Germany) using the LAS (v. 3.8) digital imaging system. Images of forewings (n = 20) and hind tibias (n = 20) were collected for the measurement of forewing size and hind tibia length using ImageJ (v. 1.47). Images of compound eyes were taken by Tabletop Microscope TM-1000 (Hitachi, Tokyo, Japan).

QUANTIFICATION AND STATISTICAL ANALYSIS

Statistical analysis was performed using SPSS (V. 22) or GraphPad Prism (v. 8.0.1). Chi-Square tests or unpaired two-tailed Student's *t*-tests were carried out where applicable. Data are presented as mean ± standard error of the mean (SEM) for three independent biological replicates. Significance levels are indicated as $*P < 0.05$, $**P \leq 0.01$, $***P \leq 0.001$, and $****P \leq 0.0001$.